Interferometric output coupling of ring optical oscillators

S. Chaitanya Kumar,[1,*] A. Esteban-Martin,[1] and M. Ebrahim-Zadeh[1,2]

[1]*ICFO-Institut de Ciencies Fotoniques, Mediterranean Technology Park, 08860 Castelldefels, Barcelona, Spain*

[2]*Institucio Catalana de Recerca i Estudis Avancats (ICREA), Passeig Lluis Companys 23, Barcelona 08010, Spain*

Corresponding author: chaitanya.suddapalli@icfo.es

Received January 7, 2011; revised February 15, 2011; accepted February 20, 2011;
posted February 24, 2011 (Doc. ID 140799); published March 17, 2011

We demonstrate the successful deployment of an antiresonant ring (ARR) interferometer within a ring optical resonator and its use for absolute optimization of output power. The integration of the ARR interferometer in a folded arm of the ring oscillator provides continuously variable output coupling over broad spectral range and under any operating conditions. We demonstrate the technique using a picosecond optical parametric oscillator (OPO), where we show continuously adjustable output coupling and optimization of the output power for different pump power conditions, from 3.5 W to 13.5 W. By operating the OPO under an optimized output coupling at 14 W of pump power, we obtain >5 W of extracted signal power, more than 2.6 times that with a ~5% conventional output coupler. We also show that the inclusion of the ARR interferometer has no detrimental effect on the spatial, temporal, and spectral characteristics of OPO output.

OCIS codes: 140.3325, 120.3180, 190.4970, 190.7110.

Since the invention of the laser in 1960, the conventional technique for maximizing output power from laser oscillators has relied on the use of a partially transmitting mirror as an output coupler. While this technique has been effective and universally deployed in all optical oscillators, absolute maximization of output power is generally impossible, because of the discrete value of mirror transmission. Moreover, optimization of output power requires trial of various output couplers with different transmission values—an empirical approach, which can be time consuming and costly [1]. Furthermore, new mirrors of different transmission values are required when variations in operating conditions, such as pumping level, alter the optimum value of output coupling.

Recently, we demonstrated a new method for absolute optimization of output power from optical oscillators based on the use of an antiresonant ring (ARR) interferometer as an output coupler [2]. Basically, the ARR consists of a beam splitter (BS), with a transmittance T and reflectance R, and a pair of high-reflectivity mirrors, which form the ring. An incident optical beam is split into two counterpropagating waves using a BS, and, after recombination at the BS, the power reflected back is given by $R_{\mathrm{ARR}} = 4RT$, while the power transmitted out of the ring is given by $T_{\mathrm{ARR}} = |R - T|^2$, implying that the reflected fields interfere in phase, whereas the transmitted fields are of opposite phase. This simple, yet powerful, technique operates over a wide wavelength range, is inherently stable, and permits arbitrary adjustment of output coupling with a simple setup by simply varying the T:R ratio of the BS in the interferometer through changes in the angle of incidence, θ_{BS}. Moreover, the ARR can be readjusted when variations in operating conditions, such as pumping level, alter the optimum value of output coupling. We reported the first realization of this concept in a femtosecond optical parametric oscillator (OPO) [2]. However, the technique was proposed only for standing-wave cavities by operating the ARR interferometer as a retro-mirror with variable transmission, thus precluding the use of the concept in unidirectional ring oscillators. As such, the exploitation of this concept in ring oscillators could not be considered a clear possibility. On the other hand, the deployment of ring resonators can offer many advantages, for example in the attainment of single-frequency operation in laser oscillators, in nonlinear resonators including OPOs, where the round-trip cavity loss can be reduced by half while maintaining the same single-pass gain, or in internal nonlinear frequency conversion experiments when unidirectional output is desired. Moreover, the implementation of the ARR in ring cavities may well extend all applications suggested in the laser context [3,4], including cavity dumping, Q switching, mode locking, nonlinear spectroscopy, and fiber optics.

In this Letter we demonstrate, for the first time to our knowledge, the use of this novel concept in a ring resonator by integrating an ARR interferometer inside a picosecond OPO based on MgO:PPLN to optimize the output coupling at different pumping levels, resulting in maximum output power for an optimum output coupling of ~42.8%($\theta_{\mathrm{BS}} = 35°$), generating more than 5 W of signal power at 1529 nm for a pump power of 14 W.

There are two key factors in the realization of the ARR concept in a ring cavity. On one hand, the use of a folded ring cavity [5] provides an almost linear cavity arm inside the main ring. On the other hand, the flexibility of the ARR to slightly misalign its feedback in a controlled manner enables us to close the folded ring. A schematic of the experimental setup is shown in Fig. 1. The pump laser is a Yb fiber laser (Fianium, FP1060-20) delivering ~20.8 ps pulses at 81.1 MHz repetition rate at 1064 nm with a double-peak spectral bandwidth of 1.38 nm (FWHM). The nonlinear crystal is a 50 mm long, 8.2 mm wide, 1 mm

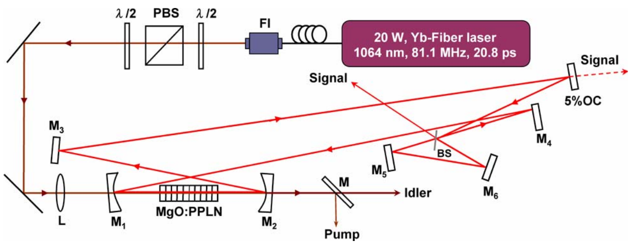

Fig. 1. (Color online) Configuration of ARR output-coupled synchronously pumped picosecond OPO in a ring cavity. L, lens; PBS, polarizing beam splitter; FI, Faraday isolator.

0146-9592/11/071068-03$15.00/0

thick 5%-doped MgO:PPLN crystal, which contains seven equally spaced grating periods ranging from 28.5 to 31.5 μm, and is housed in an oven with a temperature stability of ± 0.1 °C, as used previously in standing-wave cavity [6]. The pump beam is focused to a waist radius of $w_0 \sim 45\,\mu$m at the center of the MgO:PPLN crystal, corresponding to a confocal focusing parameter $\xi \sim 1.94$. In this work, the OPO is configured in a folded ring cavity, incorporating an ARR in the folded arm. The OPO consists of two curved mirrors, M_1 and M_2($r = 200$ mm, CaF_2 substrate), and four plane mirrors, M_3–M_6. All mirrors are highly reflecting ($R > 99\%$) for the signal over 1.3–2.2 μm and highly transmitting for the pump ($T > 90\%$) at 1064 nm and idler ($T > 87\%$) over 2.2–4 μm, thus ensuring singly resonant oscillation. A conventional plane output coupler (OC) with partial transmission ($T \sim 5\%$) over the signal wavelength range is used to extract the signal power from the OPO, and a dichroic mirror, M, separates the generated idler from the pump. A BS and the two plane mirrors M_5, M_6 constitute the ARR interferometric OC. The total optical length of the OPO ring cavity, including the 29 cm long ARR, is ~370 cm, corresponding to a repetition rate of 81.1 MHz, ensuring synchronization with the pump laser.

In order to characterize the OPO, we tuned the signal to 1529 nm by changing the temperature of the crystal to 115 °C for a grating period of 30 μm. The corresponding idler wavelength is 3498 nm. Initially we characterized the ARR interferometer outside the folded ring-cavity OPO at 1529 nm to estimate the output coupling from ARR as a function of the BS angle (θ_{BS}), using the conventional 5% OC. The ARR is then incorporated in the folded arm of the ring cavity of the OPO to realize a variable OC. The signal output is extracted from both the conventional OC and from the ARR. Signal output from the 5% OC is used as a reference, whereas ARR provides the variable output coupling to be studied. We performed optimization of signal output power at two different pump powers. Figure 2 shows the signal output power optimization as a function of output coupling from the ARR at a pump power of 13.5 W [Fig. 2(a)] and 4.5 W [Fig. 2(b)]. Also shown in the inset of Fig. 2(b) is the transmission of the ARR as a function of BS angle, θ_{BS}. As can be seen, the output coupling can be adjusted continuously from 20%, which is the minimum output coupling achieved with our BS, to very high values up to $>70\%$ by simply changing the angle, θ_{BS}, from 55° to 15°. For a fixed pump power, the signal power from ARR as well as the conventional OC is recorded by changing the angle of the BS.

As also evident from Fig. 2(a), for a fixed pump power of 13.5 W, the extracted signal power increases from 4.2 W for an output coupling value of ~20.8%($\theta_{BS} = 55°$) up to 5.1 W for an output coupling of ~42.8% ($\theta_{BS} = 35°$), beyond which it decreases, implying an optimum output coupling for this pump power, while the signal power from the 5% OC continuously decreases from 344 mW to 228 mW as the ARR output coupling varies from ~20.8%($\theta_{BS} = 55°$) to ~72.7%($\theta_{BS} = 15°$). The steady drop in the extracted signal power from the conventional OC validates the improvement in extracted signal power due to output coupling optimization by ARR and not because of the successive ARR and OPO realignment. Figure 2(b) shows the output coupling optimization of signal from the ARR at a low pump power of 3.5 W, where the extracted signal power varies from 1.28 W at ~20.8% output coupling to 1.67 W at an optimum output coupling of ~27%($\theta_{BS} = 45°$), beyond which it decreases. Again, the signal power from the conventional OC is measured to be decreasing from 121 mW to 49 mW as the ARR output coupling varies from ~20.8%($\theta_{BS} = 55°$) to ~72.7%($\theta_{BS} = 15°$). Also to be noted is the shift in the optimum value of output coupling from ~42.8%($\theta_{BS} = 35°$) for 13.5 W of pump power to ~27%($\theta_{BS} = 45°$) for 3.5 W of input pump. Moreover, the output coupling optimization curve is steeper for lower pump power than at higher pumping level. Hence, the ARR interferometer incorporated in a ring cavity enables the possibility of optimizing the output coupling at different pumping levels.

We have also studied power scaling of the ARR output-coupled OPO at the optimum output coupling

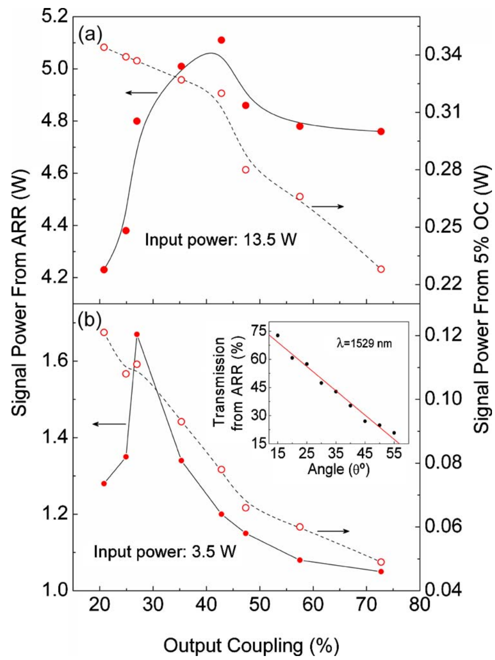

Fig. 2. (Color online) Optimization of signal power at (a) 13.5 W and (b) 3.5 W of pump power.

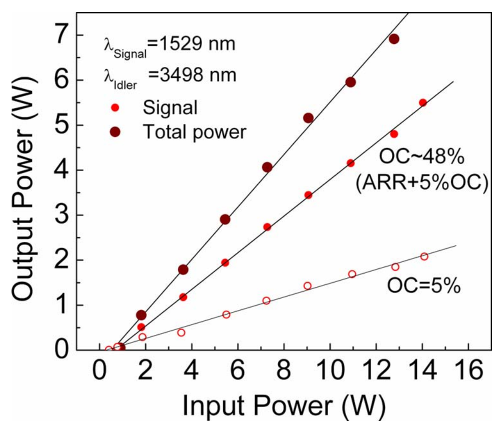

Fig. 3. (Color online) Variation of extracted signal power from the OPO using 5% conventional OC, optimum ARR output coupling along with total power from ARR as a function of the input pump power.

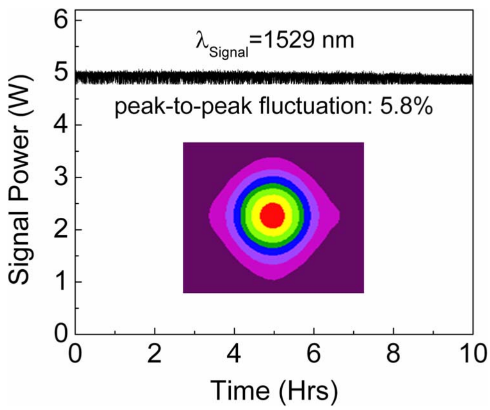

Fig. 4. (Color online) Long-term power stability and spatial profile of OPO signal pulses extracted through the ARR OC.

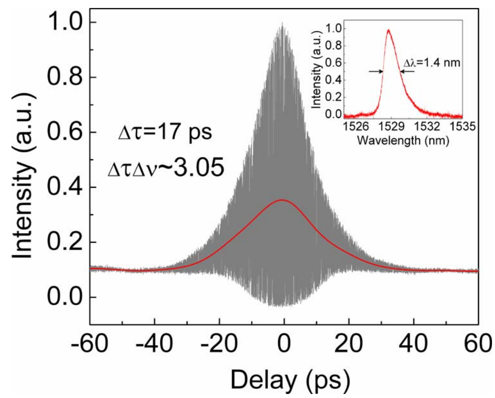

Fig. 5. (Color online) Interferometric autocorrelation of OPO signal pulses extracted trough the ARR. Inset: corresponding signal spectrum centered at 1529 nm.

of $\sim 42.8\% (\theta_{BS} = 35°)$ for high pump power. Figure 3 depicts the variation of the signal power extracted through the conventional 5% OC and the ARR OC as a function of input pump power. Also shown is the variation of the total power (signal plus idler) versus pump power at the optimum ARR output coupling. Owing to the high output coupling (~48%), the OPO threshold is 814 mW, while the threshold with conventional 5% OC is 90 mW.

However, a total signal power of 5.5 W (5.18 W from the ARR and 0.32 W from the OC) at 1529 nm, along with an idler power of 2.4 W at 3498 nm, resulting in a total power (signal plus idler) of ~8 W, is extracted from the OPO for 14 W of pump power using optimum ARR output coupling. This is while using the conventional 5% OC results in a total extracted power of only 3.45 W (2.08 W signal plus 1.37 W idler) for a similar pump power. Hence the optimization of the output coupling by incorporating ARR in our OPO has resulted in >55% improvement in the total extracted power. We have also recorded a pump depletion of >60% at the optimum ARR output coupling for 14 W of pump power. Further, we have recorded the long-term signal power stability at the optimum ARR output coupling at an extracted signal power of ~5 W, resulting in a peak-to-peak power fluctuation of 5.8% over 10 h, as shown in Fig. 4, implying a very good performance. Also shown in the inset of Fig. 4 is the signal beam profile, indicating TEM_{00} spatial mode. Using a focusing lens and a scanning beam profiler, we measured the quality factor of the output beam from the ARR output-coupled OPO to be $M_{x^2} \sim 2.3$ and $M_{y^2} \sim 1.6$ for the signal (1529 nm) and $M_{x^2} \sim 1.5$ and $M_{y^2} \sim 1.4$ for the idler (3498 nm) at full output power.

Finally, we have also performed spectral and temporal characterization of signal pulses from the ARR output-coupled OPO. Figure 5 shows the typical interferometric autocorrelation, with signal pulse duration of $\Delta\tau \sim 17$ ps. These measurements of the signal pulses correspond to a time–bandwidth product $\Delta\upsilon\Delta\tau \sim 3.05$, which is ~2.5 times lower than that of the pump pulses, indicating no degradation in the output pulse characteristics. The corresponding signal spectrum with a FWHM bandwidth of 1.4 nm, centered at 1529 nm, is shown in the inset of Fig. 5. These measurements are also similar to the results obtained with the same OPO in a standing-wave cavity using conventional OC [6], further validating the excellent performance of the ARR output coupling technique.

In conclusion, we have demonstrated, for the first time to our knowledge, a powerful and universal yet simple and practical technique for absolute optimization of output power from ring optical oscillators, providing broad bandwidth variable output coupling without any spatial, temporal, or spectral degradation of the output beam. This technique is generic and can be implemented in any type of oscillator, opening up new avenues in the context of OPOs, as well as the wider field of laser technology.

This research was supported by the European Union Seventh Framework Program MIRSURG (224042), the Ministry of Science and Innovation, Spain, through Consolider Program, SAUUL (CSD2007-00013), and by the European Office of Aerospace Research and Development (EOARD) through grant FA8655-09-1-3017.

References

1. S. Chaitanya Kumar, R. Das, G. K. Samanta, and M. Ebrahim-Zadeh, Appl. Phys. B **102**, 31 (2011).
2. A. Esteban-Martin, O. Kokabee, and M. Ebrahim-Zadeh, Opt. Lett. **35**, 2786 (2010).
3. A. E. Siegman, IEEE J. Quantum Electron. **9**, 247 (1973).
4. A. E. Siegman, IEEE J. Sel. Top. Quantum Electron. **6**, 1389 (2000).
5. W. S. Pelouch, S. Herrera, L. A. Schlie, P. E. Powers, and C. L. Tang, Proc. SPIE **2116**, 66 (1994).
6. O. Kokabee, A. Esteban-Martin, and M. Ebrahim-Zadeh, Opt. Lett. **35**, 3210 (2010).